

Submitted to *The Astrophysical Journal Letters* on 06/21/01

An Evolutionary Scenario for Blazar Unification

M. Böttcher¹

*Department of Physics and Astronomy, Rice University, MS 108,
6100 S. Main Street, Houston, TX 77005 - 1892, USA*

mboett@spacsun.rice.edu

and

C. D. Dermer

*E. O. Hulbert Center for Space Research, Code 7653,
Naval Research Laboratory, Washington, DC 20375-5352*

dermer@gamma.nrl.navy.mil

ABSTRACT

Blazar subclasses ranging from flat-spectrum radio quasars (FSRQs) through low-frequency-peaked BL Lac objects (LBLs) to high-frequency-peaked BL Lac objects (HBLs) exhibit a sequence of increasing spectral hardness with decreasing luminosity that cannot be explained solely by orientation effects. Using an analytic model for the synchrotron, synchrotron-self-Compton, and Compton-scattered external radiation from blazar jets, we propose an evolutionary scenario that links these blazar subclasses in terms of a reduction of the black-hole accretion power with time. As the circumnuclear material accretes to fuel the central engine, less gas and dust is left to scatter accretion-disk radiation and produce an external Compton-scattered component in blazar spectra. This evolutionary trend produces the sequence FSRQ → LBL → HBL. Such a scenario may also link radio-loud AGNs with ultraluminous infrared galaxies and optical QSOs, if the latter constitute the high Eddington-ratio epoch of supermassive black hole growth, as suggested by the observed anti-correlation between radio and soft X-ray activity in some Galactic black-hole candidates.

Subject headings: galaxies: active — gamma-rays: theory

¹Chandra Fellow

1. Introduction

During the past decade, significant progress has been made in understanding the physics of active galactic nuclei (AGN) and the connection between different subclasses of AGN. In particular, various lines of evidence indicate that FR II radio galaxies are the parent population of radio-loud quasars, with the relativistic jets of FSRQs being closely aligned to our line-of-sight (for a review, see Urry & Padovani (1995)). Orientation effects are also thought to unify FR I radio galaxies with BL Lac objects. The BL-Lac/FR-I subclasses have lower average luminosities than the FSRQ/FR-II subclasses. Among blazars, which include highly polarized and optically violently variable quasars, FSRQs and BL Lac objects, there appears to be an almost continuous sequence of properties from FSRQs through LBLs to HBLs. This trend is characterized by decreasing bolometric luminosities, a shift of the peak frequencies of their broadband spectral components towards higher values, and a decreasing fraction of power in γ rays compared with lower-frequency radiation (Sambruna, Maraschi, & Urry 1996; Fossati et al. 1998).

In the framework of relativistic jet models, the low-frequency (radio – optical/UV) emission from blazars is interpreted as synchrotron emission from nonthermal electrons in a relativistic jet. The high-frequency (X-ray – γ -ray) emission is thought to be produced via Compton upscattering of low frequency radiation by the same electrons responsible for the synchrotron emission. Possible sources of soft seed photons for Compton scattering are the synchrotron photons themselves (Maraschi, Ghisellini, & Celotti 1992; Bloom & Marscher 1996) or external photons, presumably dominated by the accretion disk emission which can enter the jet either directly (Dermer, Schlickeiser, & Mastichiadis 1992; Dermer & Schlickeiser 1993) or after reprocessing by circumnuclear gas and dust (Sikora, Begelman, & Rees 1994; Dermer, Sturner, & Schlickeiser 1997). In addition, a significant contribution to the soft radiation field may also be provided by infrared emission from dust in the vicinity of the AGN (Blažejowski et al. 2000; Arbeiter, Pohl, & Schlickeiser 2001).

The blazar sequence has been studied by Ghisellini et al. (1998) using a large sample of blazar broadband spectra. They suggest that the decreasing energy density of the external radiation field leads to a decreasing amount of Compton cooling. As a result, the maximum energy in the electron distribution increases, causing the synchrotron and Compton peaks to shift to higher frequencies. This explanation for the blazar sequence was developed further by Georganopoulos, Kirk, & Mastichiadis (2001), who argue that the radiating jet plasma is outside the broad-line scattering region in weak sources and within it in powerful sources. Detailed model fits to the broadband spectra of several blazars also indicate that a decreasing contribution of the external radiation to the seed photon field reproduces the FSRQ → LBL → HBL sequence. While FSRQs generally require a dominant external Compton con-

tribution to produce the observed γ -ray emission (e.g., Sambruna et al. (1997); Mukherjee et al. (1999); Hartman et al. (2001)), HBLs can be successfully fitted with pure synchrotron self-Compton (SSC) models (e.g., Mastichiadis & Kirk (1997); Pian et al. (1998); Petry et al. (2000)). The LBL BL Lacertae appears to be intermediate between those two classes, requiring a non-negligible contribution from external Comptonization to reproduce its γ -ray spectrum (Madejski et al. 1999; Böttcher & Bloom 2000). Orientation effects certainly play a role in spectral variations among sources within a given subclass, or even to account for the blue blazar subclass (Georganopoulos 2000), but cannot explain the full range of blazar properties (Sambruna, Maraschi, & Urry 1996).

It is uncertain whether the different blazar types are connected through an evolutionary sequence, or whether they constitute limited periods of AGN activity on parallel evolutionary paths. The masses of the central black holes in radio quasars generally exceed $\sim 3 \times 10^8 M_\odot$ (Wandel 1999; Laor 2000). Similarly detailed mass determinations have so far not been possible for the lineless BL Lacertae objects. The cluster environments of FR II radio galaxies and radio quasars on the one hand, and FR I radio galaxies and BL Lacs on the other hand appear consistent with an evolution of the former into the latter class of objects (Hill & Lilly 1991; Yee & Ellingson 1993; Urry & Padovani 1995). Also, the distribution of central black-hole masses in nearby galaxies appears to extend to larger values than the distribution of radio-quasar black-hole masses (Laor 2000), consistent with some fraction of present-day giant elliptical galaxies hosting the remnants of earlier quasar activity.

Here we investigate the hypothesis that an evolutionary sequence from FSRQs to BL Lac objects explains the trend in their spectral properties. We employ a combined SSC/external Compton model for relativistic jet emission, as described in §2, and derive parameter values from the observed multifrequency signatures of FSRQs and HBLs. An evolutionary sequence connecting the respective parameter regimes is proposed in §3. We discuss our results and suggest a possible evolutionary connection between radio-loud and radio-quiet AGN classes in §4.

2. Blazar Model and Parameter Estimation

The radiating plasma is modeled by a spherical emission region of co-moving radius R_b that moves outward along the axis of the jet with bulk Lorentz factor $\Gamma = (1 - \beta_\Gamma^2)^{-1/2}$. Electrons are injected into the plasma blob with a comoving power-law distribution $Q(\gamma) = Q_0 \gamma^{-s}$, for electron Lorentz factors in the range $\gamma_1 \leq \gamma \leq \gamma_2$. The luminosity L_j corresponding to the energy input of injected particles into the jet is normalized to the accretion disk power L_D through the relation $L_j = f_j L_D = m_e c^2 \int_{\gamma_1}^{\gamma_2} d\gamma \gamma Q(\gamma)$.

Electrons lose energy through adiabatic expansion, which is treated in terms of an escape time scale $t_{\text{esc}} \equiv \eta R_b/c$ with $\eta \approx 1$, and through radiative losses. These losses are generally dominated by synchrotron and Thomson processes, so they can be parameterized by the functional form $\dot{\gamma}_{\text{rad}} = -\nu_0 \gamma^2$, where $\nu_0 = 4c\sigma_T (u_B + u_{\text{sy}} + u_{\text{ext}})/3m_e c^2$. The terms u_B , u_{sy} , and u_{ext} represent the comoving magnetic field, synchrotron, and external radiation field energy densities, respectively. If u_{ext} is dominated by reprocessed accretion-disk radiation due to circumnuclear gas and dust with a scattering optical depth τ_{repr} at a characteristic distance R_{sc} from the central source, then $u_{\text{ext}} \approx \Gamma^2 L_D \tau_{\text{repr}}/(4\pi R_{\text{sc}}^2 c)$.

Electrons injected with $\gamma \gg \gamma_{\text{cr}} \equiv c/(R_b \nu_0)$ cool rapidly prior to escape, whereas electrons injected with $\gamma \ll \gamma_{\text{cr}}$ lose only a small fraction of their energy before they escape. The competition between electron injection, cooling and escape establishes an equilibrium distribution given by

$$n_{e,eq}(\gamma) = n_{e,eq}^0 \begin{cases} (\gamma/\gamma_m)^{-p} & \text{for } \gamma_l \leq \gamma \leq \gamma_m \\ (\gamma/\gamma_m)^{-(s+1)} & \text{for } \gamma_m \leq \gamma \leq \gamma_2 \end{cases} \quad (1)$$

Two distinct radiative regimes can be defined. If $\gamma_1 < \gamma_{\text{cr}}$, most of the injected electrons cool inefficiently and the electron population is in the slow cooling regime. In this case, $p = s$, $\gamma_l = \gamma_1$, $\gamma_m = \gamma_{\text{cr}}$, and $n_{e,eq}^0 = Q_0 t_{\text{esc}} \gamma_m^{-s}/V_b$, where V_b is the blob volume. When $\gamma_1 > \gamma_{\text{cr}}$, the electron population is in the fast cooling regime, $p = 2$, $\gamma_l = \gamma_{\text{cr}}$, $\gamma_m = \gamma_1$, and $n_{e,eq}^0 = Q_0 \gamma_m^{-(1+s)}/[V_b \nu_0 (s-1)]$. The synchrotron, and external-Compton radiation emitted by these relativistic electron populations are evaluated using the formulae given by Dermer, Sturmer, & Schlickeiser (1997). The SSC radiation is calculated using the analytic solution of Tavecchio, Maraschi, & Ghisellini (1998).

In the absence of an external Compton component, we recover the SSC model used to fit data from HBLs such as Mrk 501, Mrk 421, or PKS 2155-304 (e.g., Mastichiadis & Kirk (1997); Pian et al. (1998); Tavecchio, Maraschi, & Ghisellini (1998); Bednarek & Protheroe (1999); Petry et al. (2000); Sambruna et al. (2000); Fossati et al. (2000); Kataoka et al. (2000)). The parameters in an SSC model are the Doppler factor $D = [\Gamma(1 - \beta_{\Gamma} \cos \theta_{\text{obs}})]^{-1}$, the magnetic field B , R_b , γ_1 , γ_2 , the injection luminosity L_j , and the injection spectral index s . In principal, the escape time scale parameter η could also be considered a free parameter, though we assume (see Kataoka et al. (2000)) that $\eta \approx 1$, i.e., $t_{\text{esc}} \approx R_b/c$. These studies find typical HBL parameters of $R_b \sim 10^{15} - 10^{16}$ cm, $\gamma_2 \sim 10^6$, $B \sim 0.1$ G, $D \sim 20 - 30$, and a rather broad range of injection luminosities $L_j \sim 10^{37}$ ergs s $^{-1}$ – 10^{41} erg s $^{-1}$, depending on the various model details and the individual flares that are modeled.

The addition of the external Compton component in FSRQs complicates parameter estimation. We assume that the X-ray spectra of FSRQs are dominated by the SSC process, as has been argued by various authors on the basis of spectral fitting as well as variability

considerations (e.g., Mukherjee et al. (1999); Hartman et al. (2001); Sikora et al. (2001)), while the γ -ray spectrum is dominated by the external Compton component. The peak photon energies and peak νF_ν fluxes, $\nu F_\nu = 10^{-10} F_{-10}$ ergs cm $^{-2}$ s $^{-1}$, of the Compton and synchrotron components are determined from simultaneous multiwavelength observations. In the following, photon energies are given in dimensionless units $\epsilon = h\nu/m_e c^2 = 10^n \epsilon_n$, and we define $\epsilon_B \equiv B/B_{\text{cr}} = 2.3 \times 10^{-14} B(\text{G})$. The model parameters can be estimated from the observables through the expressions

$$\epsilon_{\text{sy}} = \frac{D\epsilon_B \gamma_{\text{cr}}^2}{1+z}, \quad (2)$$

$$\epsilon_{\text{ERC}} = \frac{D^2 \epsilon_* \gamma_{\text{cr}}^2}{1+z}, \quad (3)$$

$$\epsilon_{\text{SSC}} = \frac{D\epsilon_B \gamma_{\text{cr}}^4}{1+z}, \quad (4)$$

$$(\nu F_\nu)_{\text{sy}} = \frac{V_b D^4}{4\pi d_L^2} \frac{4}{3} c\sigma_T u_B \gamma_{\text{cr}}^2 n_e f_{\text{sp}} f_{\text{sy}}, \quad (5)$$

$$(\nu F_\nu)_{\text{ERC}} = \frac{V_b D^4}{4\pi d_L^2} \frac{4}{3} c\sigma_T u_{\text{ext}} \gamma_{\text{cr}}^2 n_e f_{\text{sp}} f_{\text{ERC}}, \text{ and} \quad (6)$$

$$(\nu F_\nu)_{\text{SSC}} = R_b \frac{V_b D^4}{4\pi d_L^2} \frac{4}{3} c\sigma_T^2 u_B \gamma_{\text{cr}}^4 (n_e f_{\text{sp}})^2 f_{\text{SSC}}. \quad (7)$$

The subscripts “sy,” “SSC,” and “ERC” refer to the synchrotron, SSC, and external Compton components, respectively, and ϵ_* is the mean photon energy of the external soft photon field in the stationary frame of the AGN. The factor f_{sp} in equations (5) – (7) is a normalization factor defined through $\int_1^\infty d\gamma n_e(\gamma) \gamma^2 = \gamma_{\text{cr}}^2 n_e f_{\text{sp}}$, and f_{SSC} in equation (7) is a correction factor between the νF_ν peak value and the total energy output in the SSC component, which differ significantly due to the substantial spectral broadness of the SSC emission. Typically, $f_{\text{SSC}} \sim 0.1$. For the more strongly peaked synchrotron and ERC components, the corresponding correction factor is $f_{\text{sy}} \approx f_{\text{ERC}} \sim 1$.

Combining the above estimates, and defining $d_L = 10^{28} d_{28}$ cm and $R_{\text{sc}} = 10^{18} R_{\text{sc},18}$ cm, we find

$$D = 3.2 \sqrt{\frac{\epsilon_{\text{ERC},2} \epsilon_{\text{sy},-7} (1+z)}{\epsilon_{*, -5} \epsilon_{\text{SSC},-1}}}, \quad (8)$$

$$B = 1.4 \sqrt{\frac{\epsilon_{\text{sy},-7}^3 \epsilon_{*, -5} (1+z)}{\epsilon_{\text{SSC},-1} \epsilon_{\text{ERC},2}}}, \text{ G} \quad (9)$$

$$L_D \tau_{\text{repr}} = 3 \times 10^{45} \frac{F_{\text{ERC},-10}}{F_{\text{sy},-10}} \frac{(1+z) R_{\text{sc},18}^2 \epsilon_{\text{sy},-7}^2 \epsilon_{*, -5}^2}{\epsilon_{\text{ERC},2}^2} \text{ erg s}^{-1}, \quad (10)$$

$$R_{\text{esc}} = 1.2 \times 10^{16} \frac{\epsilon_{\text{ERC},2}}{(1+z)\epsilon_{*,-5}} \sqrt{\frac{\epsilon_{\text{SSC},-1}}{\epsilon_{\text{sy},-7}^5}} \left(1 + \frac{F_{\text{ERC},-10}}{F_{\text{sy},-10}}\right)^{-1} \text{cm}, \quad (11)$$

$$R_b = 10^{17} \frac{d_{28}}{\sqrt{1+z}} \sqrt{\frac{F_{\text{sy},-10}^2}{F_{\text{SSC},-10}}} \sqrt{\frac{\epsilon_{*,-5}\epsilon_{\text{SSC},-1}^3}{\epsilon_{\text{ERC},2}\epsilon_{\text{sy},-7}^5}} \sqrt{\frac{(f_{\text{SSC}}/0.1)}{f_{\text{sy}}^2}} \text{cm, and} \quad (12)$$

$$f_j = 4(3-s) \frac{d_L^2 (\nu F_\nu)_{\text{sy}}}{L_D \gamma_1^{s-2} f_{\text{sy}}} \left(\frac{\epsilon_{\text{sy}}}{\epsilon_{\text{SSC}}}\right)^{-(2+s)/2} \left(\frac{\epsilon_*}{\epsilon_{\text{ERC}}}\right)^2 \left(1 + \frac{(\nu F_\nu)_{\text{ERC}}}{(\nu F_\nu)_{\text{sy}}}\right). \quad (13)$$

Note that equation (13) requires an independent estimate of γ_1 . Assuming that the optical spectrum is produced through synchrotron emission from strongly cooled electrons, the injection spectral index s can be estimated through the optical spectral index α_{opt} from the relation $s = 2\alpha_{\text{opt}}$.

The requirement that $\eta = R_{\text{esc}}/R_b \geq 1$ yields a constraint on the external soft photon energy ϵ_* from equations (11) and (12), given by

$$\epsilon_* \leq \frac{2.4 \times 10^{-6}}{(\sqrt{1+z} d_{28})^{2/3}} \frac{\epsilon_{\text{ERC},2}}{\epsilon_{\text{SSC},-1}^{2/3}} \left(\frac{\sqrt{F_{\text{SSC},-10}}}{F_{\text{sy},-10} + F_{\text{ERC},-10}}\right)^{2/3} \left(\frac{f_{\text{sy}}}{\sqrt{(f_{\text{SSC}}/10)}}\right)^{2/3}. \quad (14)$$

For the example of 3C 279, one of the best-observed EGRET-detected FSRQs, we can estimate typical values of the observables as $\epsilon_{\text{sy}} \sim 3 \times 10^{-7}$, $\epsilon_{\text{ERC}} \sim 300$, $\epsilon_{\text{SSC}} \sim 0.1$, $F_{\text{sy},-10} \approx 1$, $F_{\text{ERC},-10} \approx 5$, and $F_{\text{SSC},-10} \approx 0.5$ (see, e.g., Hartman et al. (2001)). For 3C 279, $z = 0.538$ and $d_{28} = 0.77$, and we take $\tau_{\text{repr}} = 0.1$, $\gamma_1 = 100$, and $s = 2.2$. Equation (14) then implies $\epsilon_* \lesssim 1.8 \times 10^{-6}$ assuming $\eta = 1$ (corresponding to $E \approx 1$ eV or $\nu \approx 2 \times 10^{14}$ Hz). The implications of this soft seed photon energy estimate will be discussed in §3. Other model parameter estimates based on these observables are $D = 28$, $B = 2.2$ G, $R_{\text{sc}} = 1.2 \times 10^{18} \sqrt{L_{46}(\tau_{\text{repr}}/0.1)}$ cm, $R_b = 1.7 \times 10^{15}$ cm, $f_j = 6.4 \times 10^{-4} L_{46}^{-1} (\gamma_1/100)^{-0.2}$, implying $L_j \sim 6.4 \times 10^{42} (\gamma_1/100)^{-0.2}$ ergs s⁻¹. The high-energy cut-off of both the synchrotron and the Compton components are poorly known in 3C 279 and other FSRQs, so no reliable constraint on the maximum electron energy γ_2 can be derived in the FSRQ case.

3. Evolutionary Sequence from FSRQs to HBLs

In the previous section, we obtained typical parameter values for HBLs and FSRQs. These estimates indicate that the most significant differences between model parameters of FSRQs and HBLs are found in the values of the jet luminosity L_j and the magnetic field B , which are both found to decrease by more than an order of magnitude from FSRQs to HBLs. The lack of evidence for a significant contribution of an external Compton component to the

γ -ray spectra of HBLs indicates that the energy density of the external soft photon field — parameterized through L_D , τ_{repr} , and R_{sc} — decreases by $\gtrsim 3$ orders of magnitude along the sequence of blazar types.

This suggests that an evolutionary scenario links the quasar and BL Lac subclasses of blazars through the depletion of material in the vicinity of the AGN. The FSRQ phase constitutes an early phase of blazar evolution in which the central regions of the galaxy are rich in gas and dust, leading to a high accretion rate onto the central, supermassive black hole. At the same time, the circumnuclear material efficiently reprocesses and scatters the accretion-disk radiation, leading to the observed strong optical emission lines in the broad line region and to a high energy density of the external soft photon field in the jet. Due to the limited supply of matter in the nuclear region, the average density of the circumnuclear material will gradually decrease, leading to a decreasing accretion rate and a decreasing reprocessing efficiency. If the fraction of accreted energy channeled into the relativistic outflow, f_j , and the transverse extent of the jet, R_b , do not change dramatically during this evolution, then this scenario will also lead to the required reduction of the magnetic field if B is in approximate equipartition with the nonthermal electron energy.

We have calculated a sequence of blazar spectra starting with the parameters appropriate for a typical FSRQ. The accretion-disk luminosity and the reprocessing efficiency, parameterized by the reprocessing optical depth τ_{repr} of the circumnuclear material, are then reduced. The magnetic field is chosen to be a constant fraction of the equipartition magnetic field so that $u_B = 0.1 u_e$. The resulting sequence of broadband spectra, shown in Fig. 1, provides a quantitative explanation for the observed trend of luminosities and peak photon energies in the FSRQ \rightarrow LBL \rightarrow HBL sequence (Fossati et al. 1998). It does not account for the spectral properties of specific blazars, which depend on variations of parameter values in different sources and, importantly, the angle between the direction of the jet axis and the direction to the observer. We note that the apparent minimum at $\nu \sim 10^{20}$ Hz in the FSRQ spectrum (corresponding to the $\tau_{\text{repr}} = 0.1$ curve in Fig. 1) might be filled in by an additional contribution from Compton-scattered accretion disk radiation that enters the jet directly, which has been neglected in our semi-analytic model.

Our estimate (Eq. [14]) for the average energy $\epsilon_* \approx 2 \times 10^{-6}$ of the dominant external soft photon field has interesting implications. It probably indicates that the external soft photon field is dominated by optical line emission from the partially ionized broad-line regions. The external photon field peaking at ϵ_* is unlikely to be due to Thomson scattering off free electrons in a highly ionized circumnuclear environment, since in that case ϵ_* should reflect the peak energy of the optically thick accretion disk, which would be inconsistent with the evidence for thermal excess emission, peaking at $\sim 2 \times 10^{15}$ Hz, observed in the low γ -ray

state of 3C 279 by Pian et al. (1999) and with the peak frequency of $\sim 3 \times 10^{15}$ Hz of the big blue bump seen in 3C 273 (Lichti et al. 1995) which is generally attributed to the emission from the optically thick accretion disk.

4. Discussion and Summary

The proposed evolutionary scenario provides a simple physical connection between different blazar subclasses in terms of the depletion of the accretion flow onto supermassive black holes. After an early phase of rapid black-hole growth, the time scale for this depletion is given by the matter free-fall time $t_{\text{ff}} \sim 7 \times 10^8 m_8 T_4^{-3/2}$ yr at the Bondi-Hoyle accretion radius, where m_8 is the mass of the central black hole in units of $10^8 M_\odot$ and $T = 10^4 T_4$ K is the average temperature of the circumnuclear material. This is generally shorter than the Hubble time, and gives a plausible time scale to explain a finite duration of blazar-like activity in the nuclei of elliptical galaxies. The scenario proposed here is also in accord with the X-ray faintness of giant elliptical galaxies known to contain supermassive black holes, which may be remnants of past blazar activity. The central sources in these galaxies have been successfully modeled with advection-dominated accretion flow solutions at very low accretion rates, $l \ll 1$ (Fabian & Rees 1995; Di Matteo & Fabian 1997; Di Matteo et al. 2000), suggesting a central region depleted after an earlier period of more efficient accretion.

If this picture is correct, then there should also be objects in an earlier phase of rapid black-hole growth that are accreting at rates $l \sim 1$. Following the scenario outlined by Sanders et al. (1988), this earlier stage of blazar evolution would comprise merging galaxies, infrared luminous galaxies, and radio-quiet QSOs. Accretion flows near the Eddington limit might produce optically-thick accretion disks extending all the way to the innermost stable orbit. If the phenomenology of Galactic black-hole candidates can be scaled to supermassive black holes accreting at comparable values of l , then radio jet formation should be quenched in such a mode of accretion as is observed, e.g., in GRS 1915+105 (Mirabel et al. 1998; Feroci et al. 1999; Belloni, Migliari, & Fender 2000), GX 339-4 (Fender et al. 1999; Corbel et al. 2000), and XTE J1550-564 (Corbel et al. 2001). This idea is supported by recent theoretical work that links the existence and energetics of a central advection-dominated inflow-outflow system to the formation of relativistic jets (Blandford & Begelman 1999; Becker, Subramanian, & Kazanas 2001). The ASCA detections of relativistically broadened Fe K α emission in MCG-6-30-15 (Tanaka et al. 1995) and IRAS 18325-5926 (Iwasawa et al. 1996) and the rapid X-ray variability seen in IRAS 13224-3809 and PHL 1092 (Boller 2000), suggest that at least in a number of cases an optically thick accretion disk does extend towards the innermost stable orbit. In most cases the evidence is yet inconclusive, but a

similar mode of accretion can generally not be ruled out.

The formation of radio jets in blazars and radio galaxies, if related to the formation of an advection-dominated accretion mode in the inner portions of the accretion flow, is triggered by a decreasing Eddington ratio. The decline of l might be due to a combination of a decreasing accretion rate and an increasing black-hole mass. An implication of this scenario is that the masses of the central black holes in galaxies which host BL Lacs should, on average, be greater than the masses of black holes in galaxies which host FSRQs or optical QSOs. Moreover, subclasses at earlier stages in the blazar sequence should exhibit increasingly stronger cosmological evolution. Bade et al. (1998) find evidence for negative cosmological evolution of X-ray selected BL Lac objects, and Stickel et al. (1991) find evidence for positive cosmological evolution in a radio-selected BL Lac sample, in accord with this picture.

To summarize, we have proposed an evolutionary scenario linking FSRQs, LBLs, and HBLs through gradual depletion of the circumnuclear environment of a supermassive black hole. As the accretion power declines with time, less gas and dust is available to reprocess accretion-disk radiation and produce an external Compton-scattered component in the blazar jet. Analytic formulae are given to estimate the relevant model parameters for FSRQs. We have calculated a spectral sequence for different blazar subclasses that are related through a one-parameter model defined by the optical depth of the circumnuclear matter. This scenario links radio-loud AGNs with progenitor merger galaxies and QSOs that constitute the high Eddington-ratio limit of the evolutionary sequence. In analogy with the observed anti-correlation between radio and soft X-ray activity in some Galactic black-hole candidates, these progenitor sources would accrete with large Eddington ratios, resulting in an optically-thick accretion disk that quenches relativistic jet production.

The work of MB is supported by NASA through Chandra Postdoctoral Fellowship grant PF 9-10007 awarded by the Chandra X-ray Center, which is operated by the Smithsonian Astrophysical Observatory for NASA under contract NAS 8-39073. The work of CD is supported by the Office of Naval Research.

REFERENCES

Arbeiter, C., Pohl, M., & Schlickeiser, R., 2001, A&A, submitted

Bade, N., Beckmann, V., Douglas, N. G., Barthel, P. D., Engels, D., Cordis, L., Nass, P., & Voges, W. 1998, A&A, 334, 459

Becker, P. A., Subramanian, P., & Kazanas, D., 2001, ApJ, 552, 209

Bednarek, W., & Protheroe, R. J., 1999, MNRAS, 310, 577

Beloni, T., Migliari, S., & Fender, R. P., 2000, A&A, 358, L29

Blandford, R. D., & Begelman, M. C., 1999, MNRAS, 303, L1

Blazejowski, M., et al., 2000, ApJ, 545, 107

Bloom, S. D., & Marscher, A. P., 1996, ApJ, 461, 657

Böttcher, M., & Bloom, S. D., 2000, AJ, 119, 469

Boller, T., 2000, in “New Vistas in Astrophysics”, Eds. M. M. Shapiro, R. Silberberg, T. S. Stanev, & J. P. Wefel (World Scientific), p. 143

Corbel, S., Fender, R. P., Tzioumis, A. K., Nowak, M., McIntyre, V., Durouchoux, P., & Sood, R., 2000, A&A, 359, 251

Corbel, S., et al., 2001, ApJ, 554, 43

Dermer, C. D., Schlickeiser, R., & Mastichiadis, A., 1992, A&A, 256, L27

Dermer, C. D., & Schlickeiser, R., 1993, ApJ, 416, 458

Dermer, C. D., Sturner, S. J., & Schlickeiser, R., 1997, ApJS, 109, 103

Di Matteo, T., & Fabian, A. C., 1997, MNRAS, 286, L50

Di Matteo, T., Quataert, E., Allen, S. W., Narayan, R., & Fabian, A. C., 2000, MNRAS, 311, 507

Fabian, A. C., & Rees, M. J., 1995, MNRAS, 277, L55

Fender, R. P., et al., 1999, ApJ, 519, L165

Feroci, M., Matt, G., Pooley, G., Costa, E., Tavani, M., & Belloni, T., 1999, A&A, 351, 985

Fossati, G., Maraschi, L., Celotti, A., Comastri, A., & Ghisellini, G., 1998, MNRAS, 299, 433

Fossati, G., et al., 2000, ApJ, 541, 166

Georganopoulos, M., 2000, ApJ, 543, L15

Georganopoulos, M., Kirk, J. G., and Mastichiadis, A. 2001, in Blazar Demographics and Physics, ed. C.M. Urry and P. Padovani, in press (astro-ph/0010159)

Ghisellini, G., Celotti, A., Fossati, G., Maraschi, L., & Comastri, A., 1998, MNRAS, 301, 451

Hill, G. J., & Lilly, S. J., 1991, ApJ, 367, 1

Iwasawa, K., Fabian, A. C., Mushotzky, R. F., Brandt, W. N., Awaki, H., & Kunieda, H., 1996,

Laor, A., 2000, ApJ, 543, L111

Lichti, G. G., et al., 1995, A&A, 298, 711

Hartman, R. C., et al., 2001, ApJ, 553, 683

Kataoka, J., Takahashi, T., Makino, F., Inoue, S., Madejski, G. M., Tashiro, M., Urry, C. M., & Kubo, H., 2000, ApJ, 528, 243

Madejski, G., et al., 1999, ApJ, 521, 145

Maraschi, L., Ghisellini, G., & Celotti, A., 1992, ApJ, 397, L5

Mastichiadis, A. & Kirk, J. G., 1997, A&A, 320, 19

Mirabel, I. F., Dhawan, V., Chaty, S., Rodriguez, L. F., Marti, J., Robinson, C. R., Swank, J., & Geballe, T., 1998, A&A, 330, L9

Mukherjee, R., et al., 1999, ApJ, 527, 132

Petry, D., et al., 2000, ApJ, 536, 742

Pian, E., et al., 1998, ApJ, 492, L17

Pian, E., et al., 1999, ApJ, 521, 112

Sambruna, R., Maraschi, L., and Urry, C.M. 1996, ApJ, 463, 444

Sambruna, R., et al., 1997, ApJ, 474, 639

Sambruna, R., et al., 2000, ApJ, 538, 127

Sanders, D. B., Soifer, B. T., Elias, J. H., Madore, B. F., Matthews, K., Neugebauer, G., & Scoville, N. Z. 1988, ApJ, 325, 74

Shakura, N. I., & Sunyaev, R. A., 1973, A&A, 24, 337

Sikora, M., Begelman, M. C., & Rees, M. J., 1994, ApJ, 421, 153

Sikora, M., Blażejowski, M., Begelman, M. C., & Moderski, R., 2001, *ApJ*, 554, 1

Stickel, M., Fried, J. W., Kuehr, H., Padovani, P., & Urry, C. M. 1991, *ApJ*, 374, 431

Tanaka, Y., et al., 1995, *Nature*, 375, 659

Tavecchio, F., Maraschi, L., & Ghisellini, G., 1998, *ApJ*, 509, 608

Urry, C. M., & Padovani, P., 1995, *PASP*, 107, 803

Wandel, A., 1999, *ApJ*, 519, L39

Yee, H. K. C., & Ellingson, E., 1993, *ApJ*, 411, 43

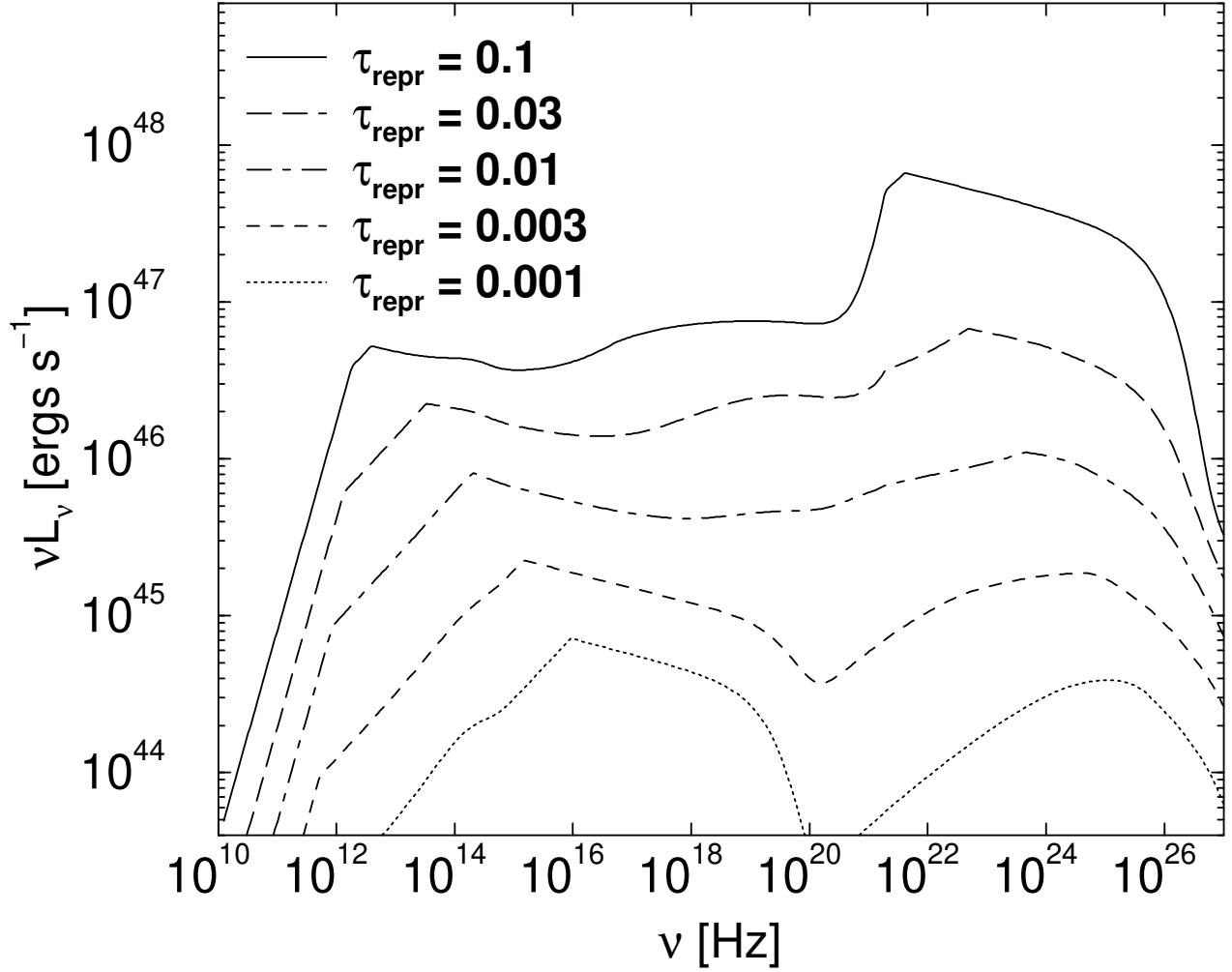


Fig. 1.— One-parameter model sequence of broadband blazar spectra that reproduces the trend in the spectral energy distributions of FSRQs, LBLs, and HBLs. Starting with typical FSRQ parameters, $\gamma_1 = 100$, $\gamma_2 = 10^6$, $s = 2.2$, $D = 28$, $R_b = 3 \times 10^{15}$ cm, $B = 2.4$ G, $L_D = 10^{46}$ ergs s^{-1} , $\tau_{\text{repr}} = 0.1$, $\epsilon_* = 10^{-6}$, $f_{\text{jet}} = 10^{-3}$, $R_{\text{sc}} = 1.2 \times 10^{18}$ cm, the sequence is generated by reducing τ_{repr} and assuming that the accretion disk luminosity is proportional to τ_{repr} . The comoving magnetic field $B = 0.3 B_{\text{ep}}$, where B_{ep} is the equipartition magnetic field with electrons.